Adsorption 8: 309–324, 2002

Analysis of Adsorption Data of Graphitized Thermal Carbon Black with a DFT-Lattice Gas Theory

D.D. DO* AND H.D. DO
Department of Chemical Engineering, University of Queensland, St. Lucia, Qld 4072, Australia
duongd@cheque.uq.edu.au

Received October 23, 2001; Revised March 14, 2002; Accepted April 19, 2002

Abstract. In this paper we analyzed the adsorption of gases and vapors on graphitised thermal carbon black by using a modified DFT-lattice theory, in which we assume that the behavior of the first layer in the adsorption film is different from those of second and higher layers. The effects of various parameters on the topology of the adsorption isotherm were first investigated, and the model was then applied in the analysis of adsorption data of numerous substances on carbon black. We have found that the first layer in the adsorption film behaves differently from the second and higher layers in such a way that the adsorbate-adsorbate interaction energy in the first layer is less than that of second and higher layers, and the same is observed for the partition function. Furthermore, the adsorbate-adsorbate and adsorbate-adsorbent interaction energies obtained from the fitting are consistently lower than the corresponding values obtained from the viscosity data and calculated from the Lorentz-Berthelot rule, respectively.

Keywords: carbon black, lattice gas theory, multi-layering adsorption, adsorbate-adsorbate interaction

1. Introduction

Adsorption equilibria have been well studied in the literature. Depending on the task of the problem at hand, there are many different approaches in dealing with adsorption equilibria. If the task is of correlation, then various empirical equations are suitable (Do, 1998). However, if the task is to provide a deeper insight about the adsorption, then various sophisticated tools, such as the Density Functional Theory (DFT) (Olivier, 1995; Olivier et al., 1994; Lastoskie and Gubbins, 2000; Lastoskie et al., 1997; Murata et al., 2001; El-Merraoui et al., 2000; Ravikovitch et al., 1998; Ravikovitch and Neimark, 2001), molecular simulations (Suzuki et al., 2000; Aoshima et al., 1999; Suzuki et al., 1999; Davies and Seaton, 2000; Heuchel et al., 1999; Lopez-Ramon et al., 1997; Turner and Quirke, 1998; Salem et al., 1998) and Lattice Gas Theory (LGT) (Tovbin, 1991; Aranovich and Donohue, 1997; Mamleev et al., 1992a, 1992b, 1992c, 1992d; Ebner, 1980), are currently available in the literature. Among these tools, the lattice gas theory is the simplest, and yet it does produce correct behavior of adsorption. Because of this simplicity, many authors have exploited the LGT to solve numerous problems in adsorption. Analysis of non-porous solid has been dealt by Tovbin (1991), Aranovich and Donohue (1997), and Mamleev et al. (1992a, 1992b, 1992c, 1992d). Many other aspects have also been considered, such as molecular heterogeneity (Aranovich and Donohue, 1996), order-disorder theory (Aranovich and Donohue, 2000a), phase loop calculation (Aranovich and Donohue, 1999a), non-random mixtures (Aranovich et al., 1997), chain molecules (Aranovich and Donohue, 1999b) and hysteresis (Aranovich and Donohue, 1998), just to name a few.

Recently, Aranovich and Donohue (2000b) studied the case where the adsorbate-adsorbate interaction in the adsorbed layer to be different from that in the bulk. They have tested a number of systems and found

*To whom correspondence should be addressed.

that there is a repulsion between molecules in the first layer. Such a repulsion is thermodynamically favorable because the increase in the free energy due to repulsion is compensated by its decrease due to the attraction to the solid surface. Here, we modify the Lattice Gas Theory and apply it in the analysis of numerous substances on non-porous graphitised carbon black where multi layers are allowed for. In the modified LGT, we assume that the behavior of the first layer is different from that of the second and higher layers. In this sense we allow for the adsorbate-adsorbate interaction energy and the partition function to be different from those of higher layers. This theory is applied to a number of adsorbates, which are representatives of noble gases, inert gases, aromatics, alkanes, alkenes, cyclic compounds, chlorinated compounds, alcohols, ethers, and water.

2. DFT-Lattice Gas Theory

2.1. Adsorbed Phase Lattice

In this section we will develop equations for adsorption based on the lattice gas theory (LGT), via the Ono-Kondo approach (Ono and Kondo, 1960). This approach was first proposed by Ono and Kondo, and it was applied quite extensively by Ebner (1980), Aranovich and Donohue (1996, 1999a, 2000a), Aranovich et al. (1997), and Aranovich and Donohue (1998, 1999b, 2000b, 2001) in the last decades in solving numerous problems in adsorption.

Here we summarize the LGT using the mean field approximation. The space above the non-porous carbon surface is divided into infinite number of lattice planes. The distance between the two adjacent lattice planes is equal to the thickness of one molecule. First we introduce some notations, which are important in the derivation of the final working equations. Let i be the i-th layer in the lattice, $E_{i,i}$ is the average interaction energy between two neighboring sites in the same layer i. $E_{i,j}$ is the average interaction energy between two adjacent sites, one of which is in the layer i while the other is in the layer j. By assuming the mean field approximation, the interaction energy between molecules in the same layer is proportional to the square of the fraction of that layer occupied by molecules, $x_i = N_i/B$, where N_i is the number of molecule in the layer i and B is the total number of lattice sites in each layer. The interaction energy between two adjacent molecules is denoted as ε. We shall assume that the lattice cell, which is a cell occupied by either a molecule or a vacancy, is a cubic cell. Therefore the interaction energy between two adjacent molecules, whether they are in the same layer or in two neighboring layers, is the same. For attraction this interaction energy ε is negative.

The interaction energy between a molecule in the layer i and the surface is denoted as $\varepsilon_{s,i}$. If the distance between the layer i and the surface is z_i, then the interaction energy between a molecule in the layer i and the surface is given by the following Steele 10-4-3 potential energy equation:

$$\varepsilon_{s,i} = \varphi_w \left[\frac{1}{5}\left(\frac{\sigma_{sf}}{z_i}\right)^{10} - \frac{1}{2}\left(\frac{\sigma_{sf}}{z_i}\right)^{4} - \frac{\sigma_{sf}^4}{6\Delta(z_i + 0.61\Delta)^3} \right] \tag{1}$$

where $\varphi_w = 4\pi\rho_s\sigma_{sf}^2\Delta\varepsilon_{sf}$.

In the mean field approximation, the average energy of interaction of neighboring sites in the same layer having the fractional coverage of x_i is:

$$E_{i,i} = \varepsilon x_i^2 \tag{2a}$$

while the interaction energy between two adjacent layers i and $i + 1$ is:

$$E_{i,i+1} = \varepsilon x_i x_{i+1} \tag{2b}$$

We shall assume that due to the influence of the vertical interaction between the solid surface and the first layer, the adsorbate-adsorbate interaction energy of the first layer is different from that of the second and higher layers. Here we have:

$$E_{1,1} = \varepsilon_1 \, x_1^2 \tag{3}$$

where ε_1 is the interaction energy of the first layer and $\varepsilon_1 \neq \varepsilon$. Knowing the interaction energy, we can write the Hamiltonian of the system as follows (Tovbin, 1991):

$$H = \sum_i \varepsilon_{s,i} x_i + z_1 \sum_i E_{i,i+1} + \frac{1}{2} z_2 \sum_i E_{i,i} + H_K \tag{4}$$

where z_1 is the coordination number between two adjacent layers, z_2 is the coordination number within the same layer, and H_K is the contribution of the kinetic energies to the total Hamiltonian. This kinetic energy

contribution is:

$$H_K = -kT \sum_i x_i \ln q_i \tag{5a}$$

where q_i is the partition function for the vibrational energy of a molecule in the i-th layer. We assume that the partition function of a molecule is the same for second and higher layers while that for the first layer is different. Hence we can write Eq. (5a) as follows:

$$H_K = -kT x_1 \ln q_1 + kT \ln q \sum_{i \geq 2} x_i \tag{5b}$$

The factor $1/2$ in Eq. (4) is introduced to avoid the counting of the pair-wise interaction in the same layer twice. The entropy of the system in the mean field approximation (Aranovich and Donohue, 1997) is:

$$S = -k \sum_i x_i \ln(x_i) - k \sum_i (1 - x_i) \ln(1 - x_i) \tag{6}$$

Therefore, the Helmholtz free energy, $F = H - TS$, can now be written as:

$$\begin{aligned} F = &\sum_i \varepsilon_{s,i} x_i + z_1 \sum_i E_{i,i+1} + \frac{1}{2} z_2 \sum_i E_{i,i} \\ &- kT x_1 \ln q_1 - kT \ln q \sum_{i \geq 2} x_i \\ &+ kT \left[\sum_i x_i \ln(x_i) + \sum_i (1 - x_i) \ln(1 - x_i) \right] \end{aligned} \tag{7}$$

The mean lattice concentrations $\{x_i\}$ are determined by minimizing the Helmholtz free energy, subject to the constraint of a fixed number of molecules in the lattice. Let N be the total number of molecules, and B be the number of lattice sites in each layer. We have the following constraint by virtue of the mass balance:

$$N = B \sum_i x_i \tag{8}$$

This problem is a classical problem of minimizing a function subject to a constraint. We can cast this problem by defining a grand potential and minimize it with respect to the lattice density. The grand potential is defined as:

$$\Omega = F - \mu \left(\sum_i x_i - \frac{N}{B} \right) \tag{9}$$

where μ is the Lagrange multiplier. Since the chemical potential is the change of the Helmholtz free energy with respect to concentration, keeping the total number of molecules constant, this Lagrange multiplier is simply the chemical potential. The solutions x_i are obtained as the solution of the following set of nonlinear algebraic equations:

$$\frac{d\Omega(x)}{dx_i} = 0 \quad \text{for } i = 1, 2, \ldots \tag{10}$$

Substituting Eq. (9b) into Eq. (10), we obtain the following set of infinite equations:

$$\begin{aligned} \mu = &\varepsilon_{s,1} + z_1 \varepsilon x_2 + z_2 \varepsilon_1 x_1 - kT \ln q_1 \\ &+ kT \ln \left(\frac{x_1}{1 - x_1} \right) \end{aligned} \tag{11a}$$

$$\begin{aligned} \mu = &\varepsilon_{s,i} + z_1 \varepsilon (x_{i-1} + x_{i+1}) + z_2 \varepsilon x_i - kT \ln q \\ &+ kT \ln \left(\frac{x_i}{1 - x_i} \right) \end{aligned} \tag{11b}$$

for $i = 2, 3, \ldots$. Equations (11) describe the lattice concentrations of all layers in terms of the chemical potential. Such a form is not useful for data analysis. Therefore, we need to relate the chemical potential in terms of the bulk pressure, which is directly measured experimentally. To achieve this, we need to consider the lattice of the bulk phase.

2.2. *Bulk Phase Lattice*

At distances far away from the surface, the lattice concentration is that of the bulk (x) and the interaction between the surface and the bulk molecule is zero, and hence the chemical potential of the bulk is derived from Eq. (11b) as written below:

$$\mu = z_0 \varepsilon x - kT \ln q + kT \ln \left(\frac{x}{1 - x} \right) \tag{12}$$

where $z_0 = 2z_1 + z_2$. The term $(-kT \ln q)$ is taken as the standard chemical potential at temperature T. Pressure is the change of the Helmholtz free energy with respect to volume, where the molar Helmholtz free energy is given by:

$$\begin{aligned} \bar{H} = &-kT \ln q + \frac{1}{2} z_0 \varepsilon x \\ &+ kT \left[\ln x + \frac{(1 - x)}{x} \ln(1 - x) \right] \end{aligned} \tag{13a}$$

from which we can derive the following expression for pressure

$$P = \frac{z_0\varepsilon}{2v_0}x^2 - \frac{kT}{v_0}\ln(1-x) \tag{13b}$$

where v_0 is the volume of a lattice unit cell.

At vapor pressure P_0, the bulk lattice concentration is x^0 and the corresponding chemical potential is μ^0, which is obtained from Eq. (12) by replacing x by x^0:

$$\mu^0 = z_0\varepsilon x^0 - kT\ln q + kT\ln\left(\frac{x^0}{1-x^0}\right) \tag{14}$$

At equilibrium, the chemical potential of the vapor phase is the same as that of the liquid phase, and since we deal with a planar interface the pressures of the gas and liquid phases are also the same. Thus if we let x_{L}^0 and x_{G}^0 be the lattice concentrations of the liquid and gas phases at equilibrium, respectively, we have the following two equations for the equality of chemical potential and pressure:

$$\begin{aligned}\mu^0 &= z_0\varepsilon x_{\mathrm{L}}^0 - kT\ln q + kT\ln\left(\frac{x_{\mathrm{L}}^0}{1-x_{\mathrm{L}}^0}\right)\\ &= z_0\varepsilon x_{\mathrm{G}}^0 - kT\ln q + kT\ln\left(\frac{x_{\mathrm{G}}^0}{1-x_{\mathrm{G}}^0}\right)\end{aligned} \tag{15a}$$

$$\begin{aligned}P_0 &= \frac{z_0\varepsilon}{2v_0}\left(x_{\mathrm{L}}^0\right)^2 - \frac{kT}{v_0}\ln\left(1-x_{\mathrm{L}}^0\right)\\ &= \frac{z_0\varepsilon}{2v_0}\left(x_{\mathrm{G}}^0\right)^2 - \frac{kT}{v_0}\ln\left(1-x_{\mathrm{G}}^0\right)\end{aligned} \tag{15b}$$

Solving Eqs. (15) for lattice concentrations at equilibrium, we get:

$$x_{\mathrm{L}}^0 + x_{\mathrm{G}}^0 = 1 \tag{16}$$

and x_{G}^0 is the smallest root of the following nonlinear equation ($0 < x_{\mathrm{G}}^0 < 1/2$)

$$\ln\left(\frac{x_{\mathrm{G}}^0}{1-x_{\mathrm{G}}^0}\right) + \frac{\varepsilon}{kT}z_0\left(x_{\mathrm{G}}^0 - \frac{1}{2}\right) = 0 \tag{17}$$

This equation only has roots when

$$-\frac{z_0\varepsilon}{kT} \geq 4 \tag{18}$$

which defines the critical temperature for the bulk lattice gas. The trivial solution of Eq. (17) is 1/2. One of the other solutions is given in the following table for various values of $z_0\varepsilon/kT$. The third solution is $x_{\mathrm{L}}^0 = 1 - x_{\mathrm{G}}^0$.

$-z_0\varepsilon/kT$	4	4.2	4.5	4.8	5.1
x_{G}^0	0.5	0.3146	0.2244	0.1707	0.1338
$-z_0\varepsilon/kT$	6	7.2	8.4	9	12
x_{G}^0	0.0707	0.0336	0.0170	0.01225	0.00255

Knowing the lattice concentration of the bulk at vapor pressure, the bulk concentration at other pressure P is obtained by subtracting Eq. (12) from Eq. (14):

$$\mu - \mu^0 = z_0\varepsilon\left(x - x_{\mathrm{G}}^0\right) + kT\ln\left[\frac{x\left(1-x_{\mathrm{G}}^0\right)}{(1-x)x_{\mathrm{G}}^0}\right] \tag{19}$$

But $\mu - \mu^0 = kT\ln(f/f_0) \approx kT\ln(P/P_0)$, and combining the above equation with Eq. (17) we derive the following equation for the lattice concentration x at any pressure $P < P_0$:

$$\ln\left(\frac{P}{P_0}\right) = \frac{z_0\varepsilon}{kT}\left(x - \frac{1}{2}\right) + \ln\left(\frac{x}{1-x}\right) \tag{20}$$

This equation now relates the bulk mole fraction in terms of pressure. When P is equal to the vapor pressure, P_0, Eq. (20) reduces to Eq. (17). As mentioned above, Eq. (17) has three roots. One is the trivial solution of 1/2, the other two solutions correspond to the gas and liquid lattice concentrations at equilibrium. For $P < P_0$, solution of Eq. (20) can yield either one solution or three solutions. When only one solution is obtained, this solution is the concentration of the bulk lattice gas. When the pressure has reached the threshold pressure, beyond which there will be three solutions. The lowest solution is the one corresponding to the lattice concentration for the gaseous phase.

2.3. *Final Working Equations*

At equilibrium, the chemical potential of the lattice sites is equal to the chemical potential of the bulk. Thus we can express the lattice concentrations to the concentration of the bulk by equating Eq. (11) to Eq. (12). As a result, we get the following equations for x_i:

$$\begin{aligned}&\ln\left[\frac{x_1(1-x)}{x(1-x_1)}\right] - \ln\left(\frac{q_1}{q}\right) + \frac{\varepsilon_{\mathrm{s},1}}{kT}\\ &\quad + \frac{\varepsilon}{kT}\left(\frac{\varepsilon_1}{\varepsilon}z_2x_1 + z_1x_2 - z_0x\right) = 0\end{aligned} \tag{21a}$$

$$\ln\left[\frac{x_i(1-x)}{x(1-x_i)}\right]+\frac{\varepsilon_{s,i}}{kT}+\frac{\varepsilon}{kT}\times(z_1x_{i-1}+z_2x_i+z_1x_{i+1}-z_0x)=0 \quad (21b)$$

for $i = 2, 3, \ldots$. Solving Eqs. (21) will give solutions for the lattice concentrations in terms of the bulk concentration x_b. One should note that the assumptions leading to the working Eqs. (21) are (i) mean field approximation, (ii) cubic lattice, (iii) constant adsorbate-adsorbate interaction within the same layer and across layer, and (iv) each molecule occupies one lattice site.

Due to these approximations, solutions to Eqs. (21) only provide approximate solution to the problem. Nevertheless it does provide a good means to obtain the various behaviors of the system (Tovbin, 1991). Depending on the pressure, the adsorption isotherm generated from solutions of Eqs. (21) could have infinite number of van der Waals loops. Due to the existence of loops, the adsorption isotherm will behave as step function in the loop region.

As we have mentioned earlier that solutions of $\{x\}$ are only in terms of the bulk concentration x. To express them in terms of the bulk pressure (or fugacity), we make use of Eq. (20) and obtain the following final working equations:

$$\frac{x_1}{1-x_1}=\left(\frac{P}{P_0}\right)\beta\exp\left[-\frac{\varepsilon_{s,1}}{kT}-\frac{\varepsilon}{kT}\times\left(\alpha z_2x_1+z_1x_2-\frac{z_0}{2}\right)\right] \quad (22a)$$

$$\frac{x_i}{1-x_i}=\left(\frac{P}{P_0}\right)\exp\left[-\frac{\varepsilon_{s,i}}{kT}-\frac{\varepsilon}{kT}\times\left(z_1x_{i-1}+z_2x_i+z_1x_{i+1}-\frac{z_0}{2}\right)\right] \quad (22b)$$

for $i = 2, 3, \ldots$. Here

$$\alpha=\frac{\varepsilon_1}{\varepsilon},\quad \beta=\frac{q_1}{q} \quad (23)$$

Knowing the lattice concentrations from Eqs. (22), the surface excess is given by:

$$\Gamma=\Gamma_m\sum_i(x_i-x_b) \quad (24)$$

3. Effects of Model Parameters

Before we discuss the applicability of the modified lattice gas model to the experimental data of many adsorbates on graphitised thermal carbon black, we first investigate the effect of various parameters on the topology of adsorption isotherm.

3.1. *Effect of the Vertical Interaction Energy*

An increase in the adsorbate-adsorbent interaction energy causes a shaper increase in the uptake. The following figure (Fig. 1) shows this effect.

The parameters used in the computation are $\Gamma_m = 3.54\ \mu$ mol/m^2, $\varepsilon_{ff}/k = 312$ K, $\alpha = 0.55$, and $\beta = 0.011$. The values for the vertical interaction energy used in this plot are 97.5, 80, 70, 60 and 50 K. The effect is strongest for the pressure range where the first layer is being formed. This is expected because the vertical interaction affects the first layer most.

3.2. *Increase in the Lateral Interaction Energy*

An increase in the lateral interaction energy, while keeping the vertical interaction energy constant, delays the condensation and hence shifts the adsorption isotherm to the right as seen in Fig. 2. This is due to the increasing importance of the adsorbate-adsorbate interaction over the adsorbate-adsorbent interaction. The parameters used in this figure are $\Gamma_m = 3.54\ \mu$ mol/m^2, $\varepsilon_{sf}/k = 97.5$ K, $\alpha = 0.55$, and $\beta = 0.011$, and the adsorbate-adsorbate interaction energy takes the following values 300, 400 and 400 K.

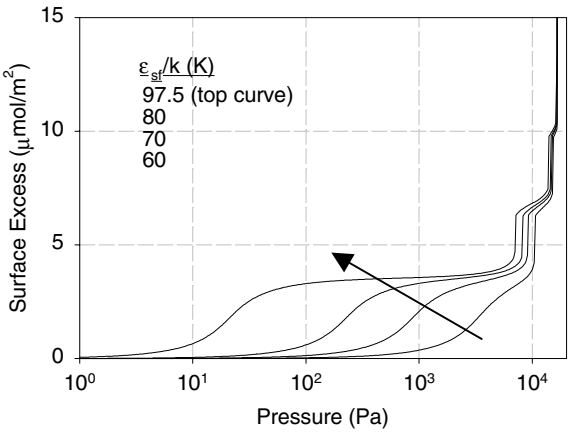

Figure 1. Effect of the vertical interaction energy on the adsorption isotherm.

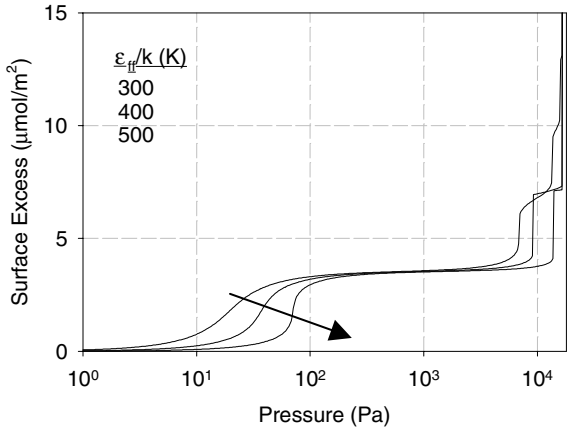

Figure 2. Effect of the lateral interaction energy on the adsorption isotherm.

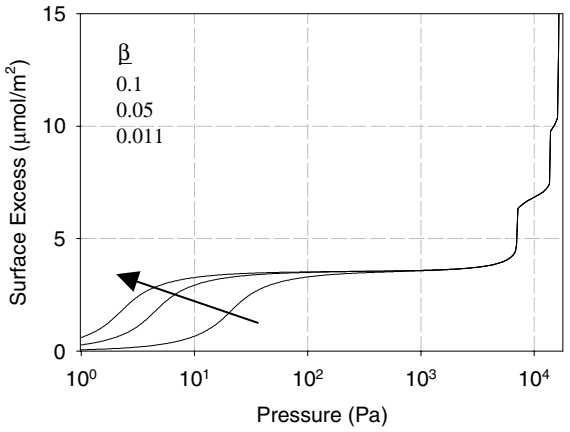

Figure 4. Effect of β on the adsorption isotherm.

3.3. Effect of α and β

The parameters α and β are defined in Eq. (23). Increase in either α or β, that is increasing the importance of the first layer, causes the sub-monolayer coverage portion of the isotherm to shift to the left, i.e. the first layer formation occurs sooner (Figs. 3 and 4). The effect of increase in α (i.e. increase in the adsorbate-adsorbate interaction energy in the first layer compared to that of other layers) causes the two-dimensional to occur in the first layer at a lower pressure, and hence a sharper increase in the isotherm portion of the monolayer. On the other hand, the increase in β causes a translational shift of the monolayer portion of the isotherm to the left (Fig. 4). On generating Figs. 3 and 4, the following base parameters have been used, $\Gamma_m = 3.54\,\mu$ mol/m^2, $\varepsilon_{\rm sf}/k = 97.5$ K, $\varepsilon_{\rm ff}/k = 312$ K, $\alpha = 0.55$, and $\beta = 0.011$.

Knowing the way how the isotherm is affected by the various parameters helps us in the process of fitting the lattice theory to the experimental data of many adsorbates onto graphitised thermal carbon black.

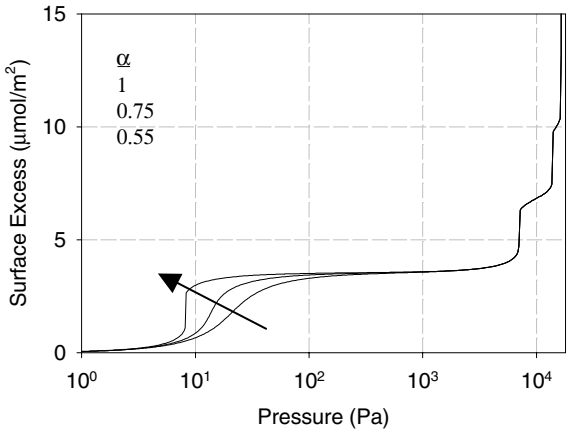

Figure 3. Effect of α on the adsorption isotherm.

4. Results and Discussions on Fitting of Carbon Black Data

4.1. Significance of the Parameters α and β

We first study the significance of the parameters α and β in the fitting. The parameter α is the ratio of the adsorbate-adsorbate interaction energy of the first layer to that of the second and higher layers (Eq. (23)). The parameter β is the ratio of the partition function of the first layer to that of the second and higher layers (Eq. (23)).

If the parameters α and β are unity, that is the behaviour of the first layer is the same as that of higher layers, Fig. 5(a) shows the fitting of benzene data at 273 K, while Fig. 5(b) shows the quality of the fitting when α and β are allowed to vary. No matter how the optimisation is carried out (different initial guess or different optimisation routines), good fitting is never achieved with α and β being unity. We also carried out the optimisation when only α is varied and $\beta = 1$ (that is the partition function of the first layer is the same as that of higher layers). A good fit is resulted but it is not as good as that when both α and β are varied. Therefore, we will allow α and β to vary in the optimisation of

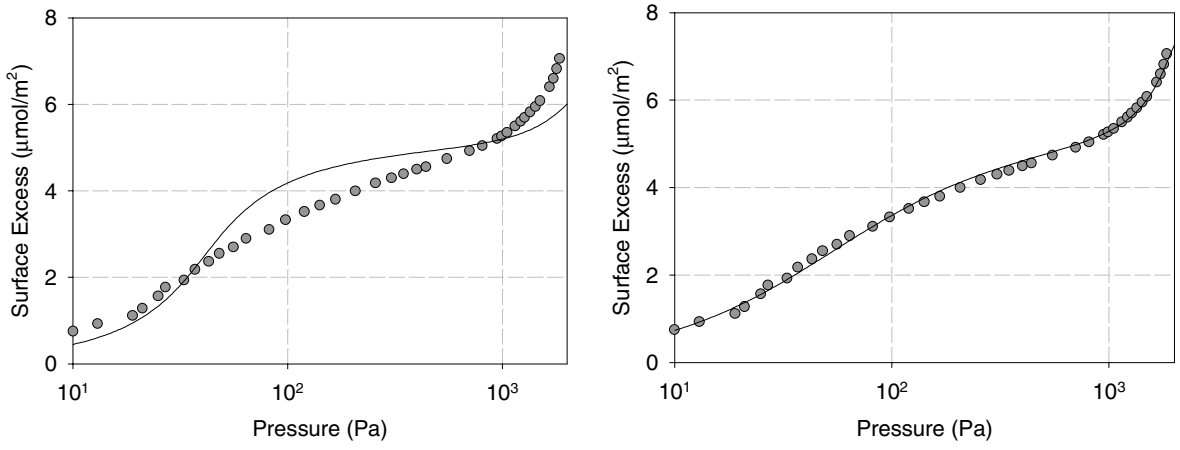

Figure 5. (a) Fitting of benzene data when $\alpha = \beta = 1$; (b) Fitting of benzene data for $\alpha = 0.113$, $\beta = 0.185$.

all adsorbates studied in this paper. The bad agreement between the theory and the experimental data when α and β are unity could be due to the surface heterogeneity, the choice of lattice structure, the rigidity of the structure, the applicability of the viscosity-derived molecular parameters in adsorption studies or the mean field approximation, etc. These factors could all contribute to the quality of the fit between the theory and the experimental data. It is difficult to delineate the relative contribution of these factors, because allowing for these factors into the model would introduce unnecessary additional parameters, which adsorption data alone may not be able to determine in a meaningful manner.

4.2. *Significance of the Long-Range Interaction of the Solid Surface*

We now investigate the effect of long range interaction of the solid surface by studying the case where only the first layer has interaction with the surface. The second and higher layers only interact with their neighbouring adsorbed layers. Like the previous section where we study the effect of α and β, in this case of only first layer interaction with the surface the good fit is never achieved, compared to the case where we allow for all layers interacting with the surface (Fig. 5(b)). When only the first layer is allowed to have interaction with the surface, the calculated isotherm does not follow a sharper turn upwards of the experimental isotherm at about 1000 Pa, at which the onset of the second layer is started. The failure of the theory to describe this second layer formation is due to the absence of long range attraction of higher layers towards the surface. Therefore subsequent fitting and calculations will be based on the model where all layers are allowed to have vertical interaction with the surface.

What to follow are the results of the fitting of the model against the experimental data of numerous vapours listed in Table 1. The molecular projection areas (column 2) are taken from Avgul and Kiselev (1970), Gregg and Sing (1982), and the molecular collision diameters (column 4) and fluid-fluid interaction energies (column 5, obtained from viscosity data) are taken from Reid et al. (1988). The theoretical monolayer coverage is calculated from:

(26)

where a_m is the molecular projection area. This is shown in Table 1 as entries in column 3. The fluid-solid interaction energy, $\varepsilon_{\mathrm{sf}}$ (column 6), is calculated from the Berthelot rule:

$$\varepsilon_{\mathrm{sf}} = \sqrt{\varepsilon_{\mathrm{ss}}\varepsilon_{\mathrm{ff}}} \tag{27}$$

The last column of Table 1 is the ratio $\varepsilon_{\mathrm{sf}}/\varepsilon_{\mathrm{ff}}$, and we note that this ratio is greatest for neon and lowest for water, suggesting the stronger adsorbate-adsorbate interaction for water than its interaction with the surface. This is what is meant by hydrophobic behaviour of water towards graphite surface.

Table 1. Properties of adsorbates used in the analysis.

	Molecular area (A^2)	$(\Gamma_m)_{\text{theoretical}}$ (μ mol/m^2)	σ_{ff} (A)	$\varepsilon_{\text{ff}}/k$ (K)	$\varepsilon_{\text{sf}}/k$	$\varepsilon_{\text{sf}}/\varepsilon_{\text{ff}}$
Neon			2.820	32.8	30.31	0.924
Argon	13.8	12.03	3.542	93.3	51.11	0.548
Krypton	15.2	10.92	3.655	178.9	70.78	0.396
Xenon	24	6.92	4.047	231.0	80.42	0.348
Nitrogen	16.2	10.25	3.798	71.4	44.71	0.626
Benzene	40	4.15	5.349	412.3	107.44	0.261
Toluene	46	3.61				
Methane	18.1	9.17	3.758	148.6	64.50	0.434
Ethane	22.7	7.31	4.443	215.7	77.71	0.360
n-Butane	40.8	4.07	4.687	531.4	121.98	0.229
iso-Butane	37.2	4.46	5.278	330.1	96.14	0.291
n-Pentane	45	3.69	5.784	341.1	97.73	0.287
n-Hexane	51	3.26	5.949	399.3	105.74	0.265
Ethylene	22.6	7.35	4.163	224.7	79.32	0.353
Cyclohexane			6.182	297.1	91.21	0.307
CCl_4	37	4.49	5.947	322.7	95.06	0.295
CF_4			4.662	134.0	61.25	0.457
Chloroform			5.389	340.2	97.60	0.287
Methanol	16	10.38	3.626	481.8	116.15	0.241
Ethanol	22	7.55	4.530	362.6	100.76	0.278
SF_6			5.128	222.1	78.86	0.355
Diethyl ether	42	3.95	5.678	313.8	93.74	0.299
Water			2.641	809.1	150.52	0.186
Ammonia			2.900	558.3	125.03	0.224
Acetone	32	5.19	4.600	560.2	125.24	0.224

What to follow are the fittings of the lattice theory against the experimental data of 26 adsorbates, which are available in the literature. The surface molar excess is calculated from Eq. (24) with the following parameters to be determined from the optimal fitting against the experimental data:

1. The monolayer coverage concentration, Γ_m (mol/m^2)
2. The scaled fluid-solid interaction energy, $\varepsilon_{\text{sf}}/k$ (K)
3. The scaled adsorbate-adsorbate interaction energy, ε/k (K)
4. The ratio of the adsorbate-adsorbate interaction energy of the first layer to that of second and higher layers, α
5. The ratio of the partition function of the first layer to that of higher layers, β

The fluid-solid interaction energy obtained from the fitting will be compared with the value calculated from the Betherlot rule , $\varepsilon_{\text{sf}} = \sqrt{\varepsilon_{\text{ss}}\varepsilon_{\text{ff}}}$, where $\varepsilon_{\text{ss}}/k = 28$ K for carbon atom and ε_{ff} is taken from the viscosity data (Reid et al., 1988). While the adsorbate-adsorbate interaction energy obtained the fitting will be compared with the fluid-fluid interaction energy ε_{ff}. This comparison will give us some ideas about the location and the compression of the adsorbed layers. This will be further discussed in the next section.

4.3. Noble Gases

4.3.1. Neon. Adsorption data of neon on carbon black P33 (2700) is available from Greyson and Aston (1957) for two temperatures 28 and 30 K. The range of pressure

Table 2. Optimal parameters for neon.

T	28 K	Units
Γ_m	20.96×10^{-6}	mole/m^2
ε_{sf}/k	21.50	K
$-\varepsilon/k$	23.11	K
α	0.35	
β	0.01	

covered is narrow (possibly due to the difficulty in conducting experiments at this low temperature) and this might result in not so reliable parameters extracted from the optimisation. We use the 28 K isotherm for the fitting, and the extracted parameters are then used to describe the adsorption isotherm at 30 K. The optimal parameters are given in Table 2, while the goodness of fit is shown in Fig. 7. The first plateau observed in the figure (labelled as M) represents the monolayer formation, of which its coverage is 21 μ mol/m^2, while the second kink observed at about 42 μ mol/m^2 represents the completion of the second layer. The projection area of neon can be calculated from the extracted monolayer coverage concentration. Assuming a densely packed monolayer, the projection area of neon is estimated to be 8 A^2. This is quite reasonable as the collision diameter of neon is 2.82 A (Reid et al., 1988), and the estimated projection area is $(2.82)^2 \approx 8$ A^2.

The extracted value for the scaled adsorbate-adsorbate interaction energy of 23 K is less than the value of 32.8 K as determined from the viscosity data (Reid et al., 1988). Similarly, the extracted scaled adsorbate-adsorbent interaction energy of 21.4 K is also less than the value of 30.31 K, calculated from the Lorentz-Berthelot rule (Eq. (26)). This behaviour of lower energy of interaction obtained from the fitting is probably due to either the over-estimation of the attractive component in the assumption of mean field approximation or the inaccuracy of the data as manifested in Fig. 6. The parameter α of 0.35 suggests that the interaction between molecules in the first layer is not as strong as those in the second and higher layers. As will be seen later, this is consistently observed for all other vapours tested in this paper. This could be due to the vertical pulling effect of the surface, resulting in weaker lateral interaction within the first layer. Furthermore, the parameter β, which is the ratio of the partition function of the first layer to that of higher layer, is also less than unity, again suggesting that molecules in the first layer are restricted in their mobility, resulted from the interaction with the surface.

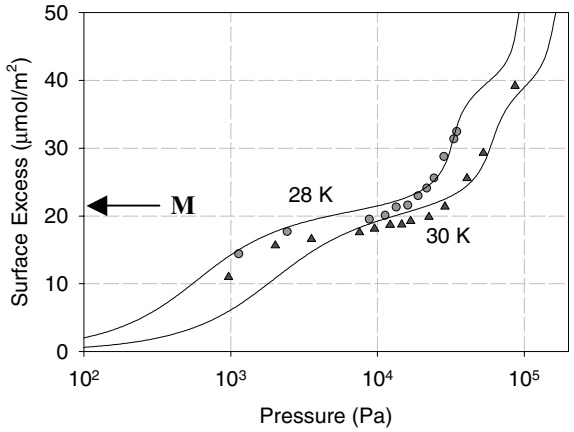

Figure 6. Fitting of neon data.

4.3.2. Argon. We next consider the argon adsorption data obtained by Ross and Winkler (1955a, 1955b) for two temperatures 77.8 and 90 K. Fitting the theory against the data of two isotherms simultaneously, we obtain the optimal parameters as tabulated in Table 3 and the fit is shown in Fig. 7. The fit of 77.8 K isotherm data is not as good as that observed for the 90 K isotherm, and this is probably due to the errors associated with the data at pressures lower than 20 Pa. Nevertheless, the temperature dependence of the adsorption isotherm is described well by the modified lattice gas model.

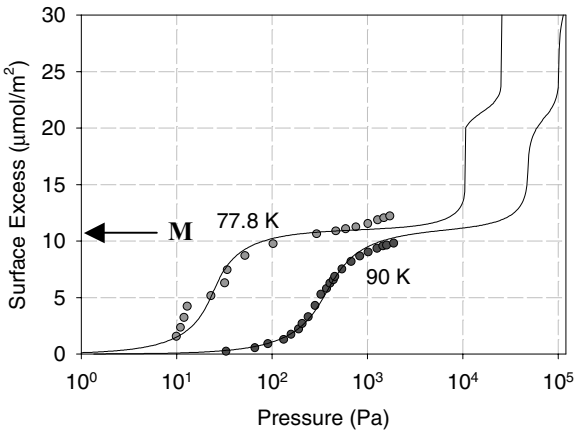

Figure 7. Fitting of argon data of Ross and Winkler.

Table 3. Comparison of interaction energies and monolayer coverage concentration.

	$(\Gamma_m)_{\text{fitted}}$ (μ mol/m^2)	$(\Gamma_m)_{\text{theo}}$ (μ mol/m^2)	$(\varepsilon_{\text{sf}}/k)_{\text{fitted}}$	$(\varepsilon_{\text{sf}}/k)_{\text{Betherlot}}$	$(\varepsilon/k)_{\text{fitted}}$	$\varepsilon_{\text{ff}}/k$ (K)	α	β
Neon	20.34		21.50	30.31	23.11	32.8	0.35	0.01
Argon	11	12.03	**48.28**	**51.11**	**86.00**	**93.3**	0.60	0.073
Krypton	10.7	10.92	63.87	70.78	131.0	178.9	0.66	0.002
Xenon	8	6.92	46.30	80.42	137.0	231.0	0.70	0.86
Nitrogen	11.22	10.25	**41.40**	**44.71**	**71.34**	**71.4**	0.288	0.269
Benzene	4.98	4.15	62.20	107.44	183	412.3	0.113	0.185
Toluene	4.3	3.61	52.20		198		0.31	0.40
Methane	10.15	9.17	44.00	64.50	110.6	148.6	0.31	0.79
Ethane	8.0	7.31	50.0	77.71	150	215.7	0.85	0.15
n-Butane	4.80	4.07	69.00	121.98	196	531.4	0.26	0.55
iso-Butane	3.60	4.46	64.80	96.14	304	330.1	0.35	0.59
n-Pentane	3.71	3.69	61.94	97.73	177	341.1	0.90	0.173
n-Hexane	3.54	3.26	97.50	105.74	312	399.3	0.552	0.011
Ethylene	7.73	7.35	71.00	79.32	148.8	224.7	0.595	0.0565
Cyclohexane	5.13		57.37	91.21	281	297.1	0.127	0.260
Carbon tetrachloride	4.70	4.49	77.70	95.06	322	322.7	0.670	0.0158
Carbon tetrafluoride	6.58		33.30	61.25	132	134.0	0.82	0.676
Chloroform	4.11		50.70	97.60	278	340.2	0.77	0.39
Methanol	15.0	10.38	71.00	116.15	430	481.8	0.63	0.31
Ethanol		7.55		100.76		362.6		
Sulfur hexafluoride	5.65		38.85	78.86	202	222.1	0.62	0.43
Diethyl ether	3.30	3.95	63.51	93.74	338	313.8	0.43	0.65
Water	4.1		79.38	150.52	551	809.1	0.56	0.98
CO_2	7.86	8.30	28	73.93	149	195.2	0.95	0.63
Ammonia	17.6		123.53	125.03	770	558.3	0.56	0.52
Acetone	8.3	5.19	76.6	125.24	271	560.2	0.69	0.063

Like the case of neon dealt with earlier, we observe the distinct formation of the first layer and the second layer characterised by the two plateaus observed in the isotherm. This characteristics of distinct plateau is observed for noble gases. The experimental data cover only the pressure range where the first layer is formed, while the model predicts the two-dimensional phase transition for the second layer. The fitted monolayer coverage concentration was found to be 11 μ mol/m^2, and this is comparable to the value of 12 μ mol/m^2, calculated from the projection area of argon of 13.8 A^2 (Lopez-Ramon et al., 1997).

Recently, Olivier (1995) obtained a comprehensive data of argon on Sterling FT-G(2700) at 87.3 K. The fit between the model and his data is shown in Fig. 8, and the optimally fitted parameters are shown in Table 3.

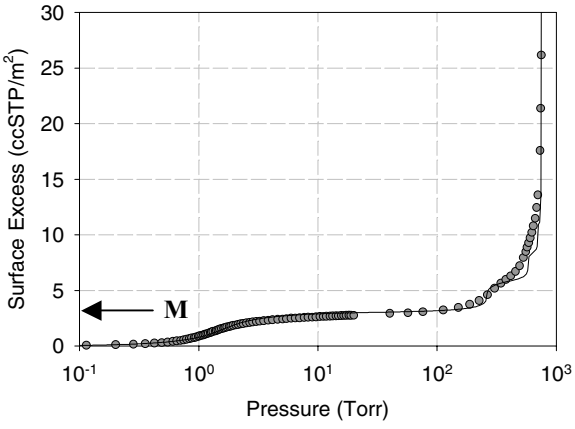

Figure 8. Fitting of argon data of Olivier.

The model shows phase transitions of the second and third layers, while the experimental data exhibits more or less smoother transition. This is possibly due to the limitations of the mean field approximation, that was discussedearlier for neon. The monolayer coverage obtained from the fitting of Olivier's data is 3.01 cc STP/g. Knowing the surface area of Sterling FT-G(2700) as 12.8 m^2/g, the monolayer coverage concentration is 10.5 μ mol/m^2, which is very comparable to the value of 11 μ mol/m^2 obtained from the analysis of Ross and Winkler's data. The scaled energy for adsorbate-adsorbate interaction extracted from the fitting is 86 K, compared closely to 93 K from the LJ-value from the viscosity data (Reid et al., 1988), while that for adsorbate-adsorbent is 48 K, which is also close to the value of 51 K calculated from the Lorentz-Berthelot rule (Eq. (27)). As will be seen later that only for argon and nitrogen that we find the extracted interaction energies are close to the LJ-value obtained from the viscosity data and that calculated from the Lorentz-Berthelot rule.

4.3.3. Krypton. We now consider the adsorption data of krypton on carbon black P33(2700) from Amberg et al. (1955). Data at 77.8 K was used in the fitting, and the results are shown below in Appendix 1. The model describes well the first and second layers formation, but the experimental formation of the third layer seems much smoother than what the model describes.

4.3.4. Xenon. The data for xenon adsorption on Sterling MT(3100) is available from Cochrane et al. (1967) at four temperatures 162, 173, 183 and 195 K. By fitting all four isotherms simultaneously, the result is satisfactory (Appendix 1).

Having analysed the adsorption data of all noble gases, we summarise the results in the Table 4. Here we see that the solid-fluid interaction energy ε_{sf} obtained from the fitting is consistently less than the value calculated from the Lorentz-Berthelot rule (Eq. (27)). This may seem to suggest that noble gas atom is probably located closer to the carbon black surface. On studying the fluid-fluid interaction energy obtained from the fitting we find that these values are also consistently lower than the molecular fluid-fluid interaction energy (Reid et al., 1988). This can be attributed to the assumption of mean field approximation. However, we note that the difference between the energies extracted from the fitting are much less than calculated values for xenon. It is not possible to draw any firm reason for this large difference because even the factors such surface heterogeneity, lattice structure, etc. have been accounted for it is expected that the values for energies are not much different from those obtained here. On the observation of the experimental data at 162 K, we see that there are scatters in the data set, and the not-so-good fit with this data set could be the reason for low energies obtained from the fitting compared to the calculated values.

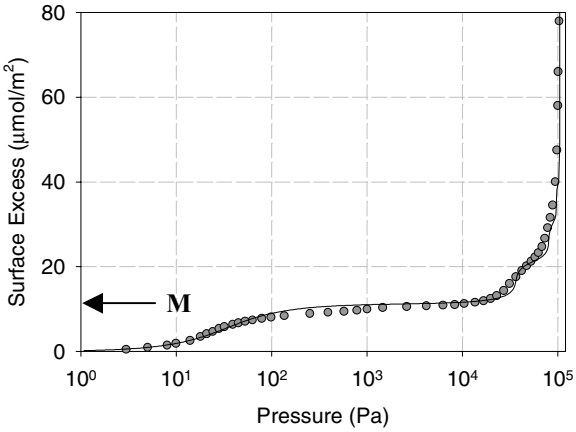

Figure 9. Fitting of nitrogen data at 77.8 K.

4.4. Nitrogen

We now turn to the most celebrated adsorptive used in the past many decades for surface area and pore size characterisation, nitrogen. Figure 9 shows the fit

Table 4.

	ε_{sf}/k (from fitting)	ε_{sf}/k (from Betherlot)	ε/k (from fitting)	ε_{ff}/k (from Reid et al. (1988))
Neon	21.5	30.3	23.11	32.8
Argon	48.28	51.1	86	93.3
Krypton	63.87	70.78	131	178.9
Xenon	46.3	80.4	137	231

between the modified lattice theory and the experimental data of Isirikyan and Kiselev (1961).

We see that the fit between the theory and data for nitrogen over many decades of pressure is excellent. The optimally fitted parameters are listed in Table 3. The monolayer coverage concentration was found to be 11.2 μ mol/m^2, which is comparable to the theoretical value of 10.3 μ mol/m^2 obtained from the projection area of 16.2 A^2 for nitrogen (Gregg and Sing, 1982). The extracted scaled fluid-solid interaction energy, ε_{sf}/k, was found to be 41.4 K, which is comparable to 44.7 K calculated from the Lorentz-Berthelot rule, suggesting that the location of the first layer of nitrogen is only slightly closer to the carbon surface. This also has been observed with all noble gases discussed earlier. We also note that the energies obtained from the fitting of argon and nitrogen are very close to the theoretical values. This could be partly attributed to their extensive data over a very wide range of pressure. This stresses the need for the reliable data collected over a wide range of pressure (and temperature) for the validation of a model.

4.5. Aromatics

We have studied the properties of the noble gases and nitrogen adsorption on carbon black, and now we turn to adsorption of aromatics on carbon black.

4.5.1. Benzene. Benzene is among the most studied adsorbates in adsorption on carbonaceous materials. We use the benzene data on carbon black P33(2700) of Pierotti and Smallwood (1966). The fit between the lattice theory and the benzene data at 273 K is shown in Fig. 5(b), where we observe an excellent fit. The optimally fitted parameters are tabulated in Table 3.

The optimally extracted parameter for the monolayer coverage, 4.98 μ mol/m^2 is larger than the theoretically calculated value of 4.2 μ mol/m^2, which may suggest that benzene molecules may not adsorb parallel to the surface. This is confirmed in a molecular study using MOPAC, a general purpose molecular orbital package (O'Dea et al., 1999). This tilting behaviour of benzene is also reflected in the value of the scaled adsorbate-adsorbent interaction energy, ε_{sf}/k. Using the Lorentz-Berthelot rule, we calculate this value as 107 K, while the optimally extracted value for this parameter is 62 K, supporting the tilting behaviour of benzene molecule against the carbon black surface.

On considering the fitted scaled adsorbate-adsorbate interaction energy, ε/k, of 183 K, we find that it is significantly less than the molecular scaled fluid-fluid interaction energy, ε_{ff}/k, of 412.3 K obtained from viscosity data. This is possibly due to the compression of the adsorbed phase, which results in slightly closer benzene molecules, leading to a lower adsorbate-adsorbate interaction energy. Another reason could be the assumption of the mean field approximation.

4.6. Other Adsorbates

We also study the fitting of the model against the data of many other adsorbates listed below:

1. Toluene at 262 and 273 K (Pierce and Ewing, 1967)
2. Methane at 262 and 273 K (Pierce and Ewing, 1967)
3. Ethane at 148 K (Avgul and Kiselev, 1970)
4. *n*-butane at 303, 315 K (Beebe et al., 1950)
5. iso-butane at 298, 323, 348 K (Hoory and Prausnitz, 1967)
6. *n*-pentane at 293 K (Avgul and Kiselev, 1970)
7. *n*-hexane at 293 K (Isirikyan and Kiselev, 1961)
8. Ethylene at 173, 183, 193 K (Bezus et al., 1964a, 1964b, 1964c)
9. Cyclohexane at 245 K (Pierce and Ewing, 1967)
10. Carbon tetrachloride at 293 K (Avgul and Kiselev, 1970)
11. Carbon tetrafluoride at 90 K (Graham, 1958)
12. Chloroform at 248, 268, 288, 297 and 323 K (Machin and Ross, 1962)
13. Methanol at 273, 293, 316 K (Belyakova et al., 1968)
14. Sulfur hexafluoride at 193 K (Beebe et al., 1964)
15. Diethyl ether at 293 K (Avgul et al., 1961)
16. Water at 302, 323 K (Belyakova et al., 1968)
17. Carbon dioxide at 193 K (Beebe et al., 1964)
18. Ammonia at 195 K (Holmes and Beebe, 1957)
19. Acetone at 303, 323 K (Ustinov, 2000)

What we have found is that we also observe the same behaviour as that observed for noble gases, nitrogen

and benzene. The results are shown graphically in Appendix 1, and the optimally fitted parameters are listed in Table 3. As seen in the figures, the model describes well the data of all adsorbates, except that of ammonia, and most of all the temperature dependence is correctly described by the model. What this means is that if the adsorption isotherm is known for one temperature, the model can be used to predict the isotherms for other temperatures.

With respect to ammonia, the model incorrectly describes the formation of the second layer. In the light that the model describes all adsorbates (other than ammonia), the deviation between the theory and the data of ammonia could be attributed to either the inaccuracy of the data or the inadequacy of the model in dealing with ammonia. The reason of hydrogen bonding between ammonia molecules is not fully justified as the model describes water adsorption reasonably well.

5. Discussions

We summarize the values of fitted parameters of interaction energies for all adsorbates studied in Table 3. For comparison, we also list the molecular fluid-fluid interaction energy, and the fluid-solid interaction energy calculated from the Lorentz-Berthelot rule.

We consistently find that in all systems investigated, the parameter α is less than unity, meaning that the adsorbate-adsorbate interaction energy of the first layer is always less than that of the second and higher layers. This could be due to the fact that molecules in the first layer are strongly pulled towards the surface, affecting the adsorbate-adsorbate interaction in such a way that it weakens the lateral interaction. Since the parameter α is found to be positive in all cases, our conclusion is that there is still attraction in the first layer. The parameter β is also less than unity, and the explanation for this is similar to that for α. For neon, krypton, *n*-hexane and carbon tetrachloride, the value of β is found be 0.01, 0.002, 0.011 and 0.0158, respectively. This suggests that the partition function of the first layer is much smaller than that of the second and higher layers. It seems unreasonable, and many factors could contribute to this, for example, the choice of lattice structure, the possibility of surface heterogeneity and the mean field approximation assumption, and the quality of the experimental data. We take neon data for example (Fig. 6). There is a lack of data in the low pressure region ($P < 1000$ Pa), and if the data in the low pressure region were greater than the theoretical curve as shown in Fig. 6, the value of β would be greater. In the absence of this as well as the questions on other factors (surface heterogeneity, lattice structure, the mean field approximation and the rigidity of the lattice structure, etc.) the model seems to describe well the data, especially the temperature dependence of the adsorption isotherm.

On comparing the fitted parameter for ε_{sf}/k and the value calculated from the Lorentz-Berthelot rule, we find in general that the fitted values are always less than the theoretical value. This may indicate that molecules are located closer to the surface. We also find that the adsorbate-adsorbate interaction energy obtained from the fitting is also less than the fluid-fluid interaction energy. This might be attributed to a number of reasons:

1. The assumption of mean field approximation, which might over-estimate the attractive force,
2. Molecules move closer to each other both laterally and vertically. In moving closer laterally more molecules can be inserted and this is favorable because the repulsion due to the closeness of adjacent molecules is compensated by the increase in attractive energy to the surface. In moving closer vertically, the repulsion due to the closeness of adjacent layers is again compensated by the increase in the attraction energy towards the surface.

Although we have said that the interaction energy ε_{sf} found from the fitting is less than the value calculated from the Lorentz-Berthelot rule and the adsorbate-adsorbate interaction energy is less than the fluid-fluid interaction energy obtained from viscosity data, we do find those corresponding values are very much comparable to each other for argon and nitrogen. This finding is interesting in the light of these two adsorbates are the most commonly used adsorptive for surface area and pore size characterization.

6. Conclusion

We have studied the analysis of numerous adsorption systems of non-porous carbon black by using a method of lattice gas. In this theory we have allowed for the

different behavior of the first layer from that of higher layers. From the fitting exercise, it was found that the adsorbate-adsorbate interaction energy of the first layer is lower than that of higher layers and so is the partition function. Furthermore, the adsorbate-adsorbate interaction energy is less than the fluid-fluid interaction energy obtained from viscosity data, and this is attributed to the pulling effect of the surface that adsorbate layers can be closer to each other, resulting in a reduction in the interaction energy. Among all adsorbates tested, we found that argon and nitrogen have their interaction energies very much comparable to the corresponding values obtained from the Lorentz-Betherlot rule and from the viscosity data.

Appendix 1

This appendix contains figures of model's fitting against the experimental data of a number of adsorbates: (a) krypton, (b) xenon, (c) toluene, (d) methane, (e) ethane, (f) *n*-butane, (g) iso-butane, (h) *n*-pentane, (i) *n*-hexane, (j) ethylene, (k) cyclohexane, (l) carbon tetrachloride, (m) carbon tetrafluoride, (n) chloroform, (o) methanol, (p) sulfur-hexafluoride, (q) diethyl ether, (r) water, (s) carbon dioxide, (t) ammonia and (u) acetone. The temperatures are shown in the bracket of the caption of each figure. For isotherms at various temperatures, the uppermost curve corresponds to the lowest temperature. The label M is to denote monolayer.

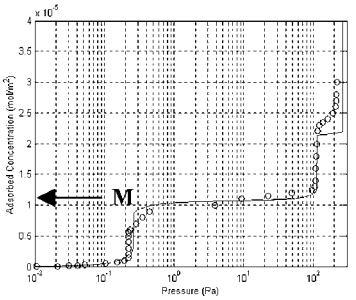

(a) *Krypton (77.8 K)*

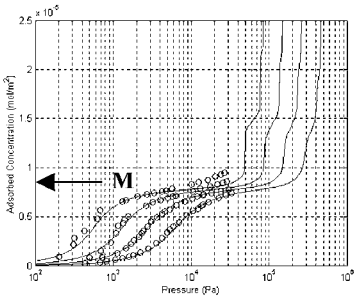

(b): *Xenon(162, 173, 183, 195 K)*

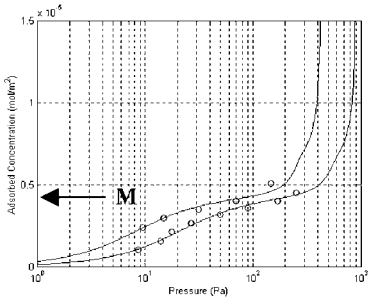

(c) *toluene (263, 273 K)*

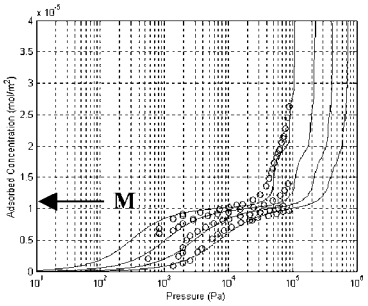

(d): *methane (113, 123, 133 and 143 K)*

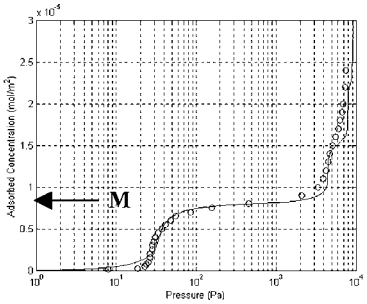

(e): *ethane (148 K)*

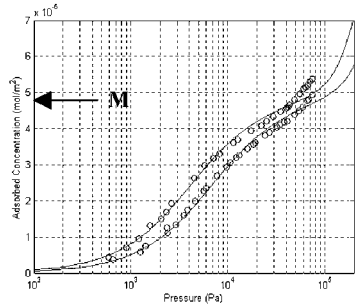

(f): *n-butane (303 and 315 K)*

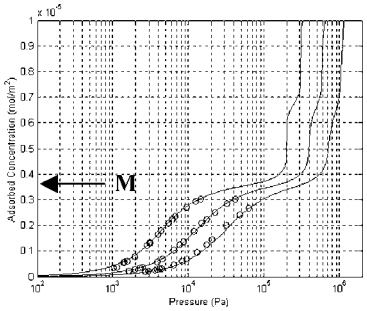

(g): *iso-butane (298, 323 and 348 K)*

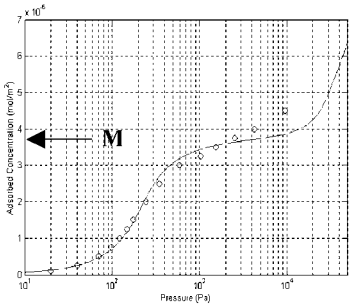

(h): *n-pentane (293 K)*

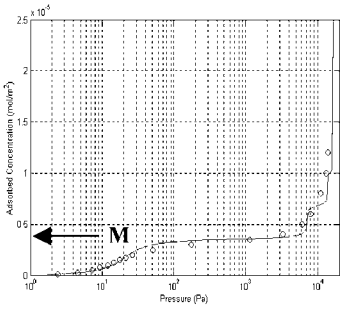

(i): *n-hexane (293 K)*

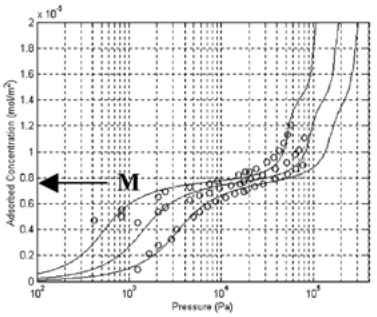

(j): ethylene (173, 183, 193 K)

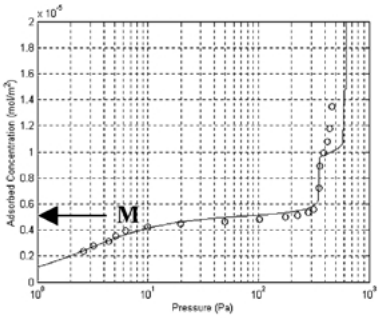

(k): cyclohexane (245 K)

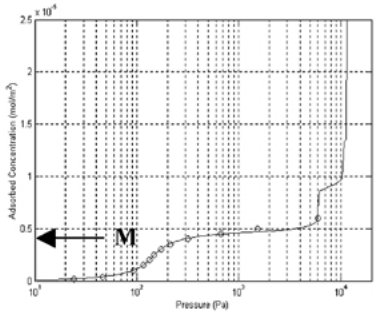

(l): carbon tetra-chloride (293K)

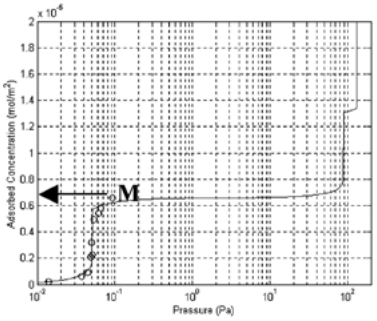

(m): *carbon tetrafluoride (90K)*

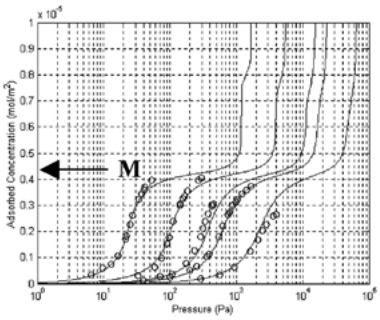

(n): *chloroform (248, 268, 288, 297, 323 K)*

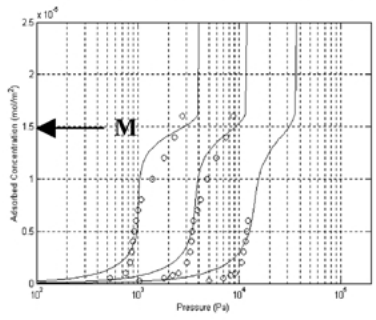

(o): *methanol (273, 293, 316 K)*

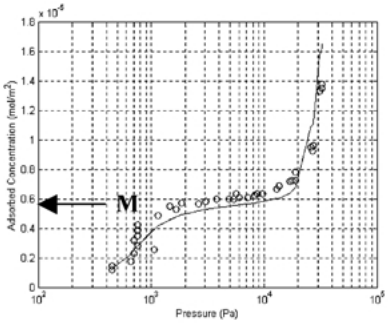

(p): *sulfurhexafluoride (193 K)*

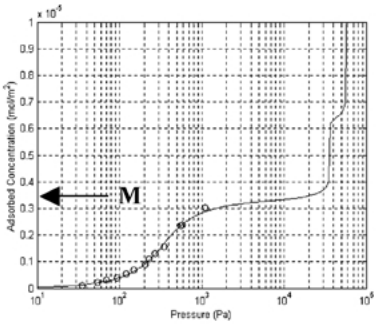

(q): *diethyl-ether (293 K)*

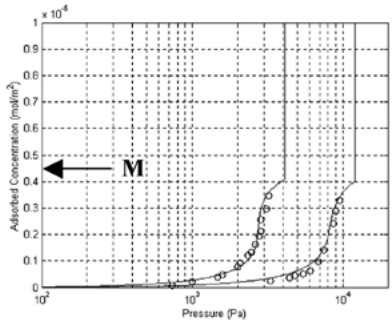

(r): *water (302, 323 K)*

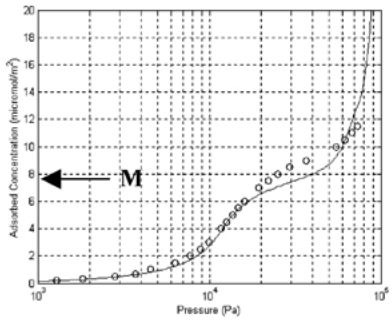

(s): *carbon dioxide (193 K)*

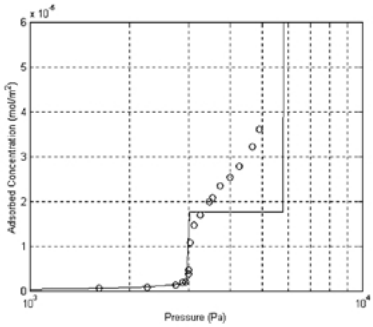

(t): *ammonia (195 K)*

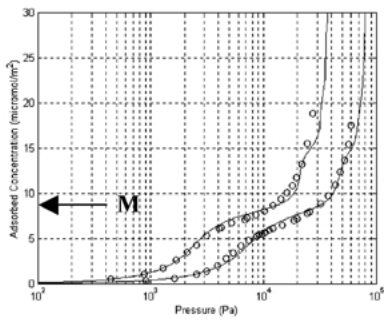

(u): *acetone (303, 323 K)*

Acknowledgment

This project is supported by the Australian Research Council.

References

Amberg, C.H., W.B. Spenser, and R.A. Beebe, *Can. J. Chem.*, **33**, 305–313 (1955).

Aoshima, M., T. Suzuki, and K. Kaneko, *Chem. Phys. Lett.*, **310**, 1–7 (1999).

Aranovich, G. and M. Donohue, *J. Chem. Phys.*, **104**, 3851–3859 (1996).

Aranovich, G. and M. Donohue, *J. Colloid Int. Sci.*, **189**, 101–108 (1997).

Aranovich, G. and M. Donohue, *J. Colloid Int. Sci.*, **205**, 121–130 (1998).

Aranovich, G. and M. Donohue, *Phys. Rev. E*, **60**, 5552–5560 (1999a).

Aranovich, G. and M. Donohue, *J. Colloid Int. Sci.*, **213**, 457–464 (1999b).

Aranovich, G. and M. Donohue, *J. Chem. Phys.*, **112**, 2361–2366 (2000a).

Aranovich, G. and M. Donohue, *J. Colloid Int. Sci.*, **227**, 553–560 (2000b).

Aranovich, G. and M. Donohue, *Colloid and Surfaces A*, **187**, 95–108 (2001).

Aranovich, G., T. Hocker, D.W. Wu, and M.D. Donohue, *J. Chem. Phys.*, **106**, 10282–10291 (1997).

Avgul, N. and A. Kiselev, *Chemistry and Physics of Carbon*, **6**, 1–124 (1970).

Avgul, N.N., A.V. Kiselev, and I.A. Lygina, *Izv. Akad. Nauk SSSR, Otd. Akad. Nauk*, 2116–2125 (1961).

Beebe, R.A., G.L. Kington, M.H. Polley, and W.R. Smith, *J. Am. Chem. Soc.*, **72**, 40–42 (1950).

Beebe, R.A., A.V. Kiselev, N.V. Kovaleva, R.F.S. Tyson, and J.M. Holmes, *Zh. Fiz. Khim.*, **38**, 708–719 (1964).

Belyakova, L.D., A.V. Kiselev, and N.V. Kovaleva, *Zh. Fiz. Khim.*, **42**, 2289 (1968).

Bezus, A.G., A.V. Kiselev, and V.P. Dreving, *Russian J. Phys. Chem.*, **38**, 1589–1593 (1964a).

Bezus, A.G., A.V. Kiselev, and V.P. Dreving, *Russian J. Phys. Chem.*, **38**, 30–35 (1964b).

Bezus, A.G., A.V. Kiselev, and V.P. Dreving, *Russian J. Phys. Chem.*, **38**, 511–515 (1964c).

Cochrane, H., P.L. Walker, Jr., W.S. Diethorn, and H.C. Friedman, *J. Coll. Interface Sci.*, **24**, 405–415 (1967).

Davies, G. and N. Seaton, *AIChE J.*, **46**, 1753–1768 (2000).

Do, D.D., *Adsorption Analysis: Equilibria and Kinetics*, Imperial College Press, London, 1998.

Ebner, C., *Physical Review A*, **22**, 2776–2781 (1980).

El-Merraoui, M., M. Aoshima, and K. Kaneko, *Langmuir*, **16**, 4300–4304 (2000).

Graham, D., *J. Phys. Chem.*, **62**, 1210–1211 (1958).

Gregg, S.J. and K.S.W. Sing, *Adsorption, Surface Area and Porosity*, Academic Press, London, 1982.

Greyson, I. and J.G. Aston, *J. Phys. Chem.*, **61**, 610–613 (1957).

Heuchel, M., G. Davies, E. Buss, and N. Seaton, *Langmuir*, **15**, 8695–8705 (1999).

Holmes, J.M. and R.A. Beebe, *J. Phys. Chem.*, **61**, 1864–1866 (1957).

Hoory, S.E. and J.M. Prausnitz, *Trans. Farad. Soc.*, **63**, 455–460 (1967).

Isirikyan, A.A. and A.V. Kiselev, *J. Phys. Chem.*, **65**, 601–607 (1961).

Lastoskie, C. and K. Gubbins, in *Characterisation of Porous Solids V*, K. Unger et al. (Eds.), Elsevier, Amsterdam, 2000.

Lastoskie, C., N. Quirke, and K. Gubbins, in *Equilibria and Dynamics of Gas Adsorption on Heterogeneous Solids*, W. Rudzinski et al. (Eds.), Elsevier, Amsterdam, 1997.

Lopez-Ramon, M., J. Jagiello, T. Bandosz, and N. Seaton, *Langmuir*, **13**, 4435–4445 (1997).

Machin, W.D. and S. Ross, *Proc. Roy. Soc.* (London), **A265**, 455–462 (1962).

Mamleev, V., L. Astapenkova, and P. Gladyshev, *Russ. J. Phys. Chem.*, **66**, 835–838 (1992a).

Mamleev, V., L. Astapenkova, and P. Gladyshev, *Russ. J. Phys. Chem.*, **66**, 979–984 (1992b).

Mamleev, V., L. Astapenkova, and P. Gladyshev, *Russ. J. Phys. Chem.*, **66**, 1144–1149 (1992c).

Mamleev, V., L. Astapenkova, and P. Gladyshev, *Russ. J. Phys. Chem.*, **66**, 1606–1612 (1992d).

Murata, K., M. El-Merraoui, and K. Kaneko, *J. Chem. Phys.*, **114**, 4196–4205 (2001).

O'Dea, A., R.S. Smart, and A.R. Gerson, *Carbon*, **37**, 1133 (1999).

Olivier, J., *J. Porous Materials*, **2**, 9–17 (1995).

Olivier, J., W. Conklin, and M. Szombathely, in *Characterisation of Porous Solids III*, J. Rouquerol, F. Rodriguez-Reinoso, K. Sing, and K. Unger (Eds.), Elsevier, Amsterdam, 1994.

Ono, S. and S. Kondo, "Molecular Theory of Surface Tension in Liquids," in *Encyclopedia of Physics*, S. Flugge (Ed.), Vol. X, pp. 134–277, 1960.

Pierce, C. and B. Ewing, *J. Phys. Chem.*, **71**, 3408–3413 (1967).

Pierrotte, R.A. and R.E. Smallwood, *J. Coll. Interface Sci.*, **22**, 469–481 (1966).

Ravikovitch, P., G. Haller, and A. Neimark, *Adv. Coll. Int. Sci.*, **76**, 203–226 (1998).

Ravikovitch, P. and A. Neimark, *Coll. Surfaces A*, **187**, 11–21 (2001).

Reid, R.C., J.M. Prausnitz, and B.E. Poling, *The Properties of Gases and Liquids*, McGraw Hill, New York, 1988.

Ross, S. and W. Winkler, *J. Coll. Sci.*, **10**, 319–329 (1955a).

Ross, S. and W. Winkler, *J. Coll. Sci.*, **10**, 330–337 (1955b).

Salem, M., P. Brauer, M. Szombathely, M. Heuchel, P. Harting, K. Quitzch, and M. Jaroniec, *Langmuir*, **14**, 3376–3389 (1998).

Suzuki, T., T. Iiyama, K. Gubbins, and K. Kaneko, *Langmuir*, **15**, 5870–5875 (1999).

Suzuki, T., R. Kobori, and K. Kaneko, *Carbon*, **38**, 623–641 (2000).

Tovbin, Yu. K. *Theory of Physical Chemistry Processes at a Gas-Solid Interface*, CRC Press, 1991.

Turner, A. and N. Quirke, *Carbon*, **36**, 1439–1446 (1998).

Ustinov, E., *Adsorption*, **6**, 195–204 (2000).